Sustainable Chemistry and Pharmacy 35 (2023) 101132

Contents lists available at ScienceDirect

Sustainable Chemistry and Pharmacy

journal homepage: www.elsevier.com/locate/scp

Aqueous biphasic systems comprising analogues of glycine-betaine ionic liquids: Toward greener separation platforms

Inês S. Cardoso [a], Filipe H.B. Sosa [a], Armando J.D. Silvestre [a], Anthony Robert [b], Mara G. Freire [a, *], Aminou Mohamadou [b, **]

[a] CICECO – Aveiro Institute of Materials, Department of Chemistry, University of Aveiro, Campus Universitário de Santiago, 3810-193 Aveiro, Portugal
[b] Institut de Chimie Moléculaire de Reims (ICMR), UMR CNRS 7312, Université de Reims Champagne-Ardenne, Moulin de la Housse, BP 1039, 51687, Reims cedex 2, France

ARTICLE INFO

Handling Editor: Fabio Aricò

Keywords:
glycine-betaine ionic liquids
Thermal properties
Ecotoxicity
Aqueous biphasic systems
Binodal curves
Extraction

ABSTRACT

The use of biobased and bioactive compounds has boosted the development of sustainable extraction and purification processes, in which ionic liquids have been playing a major role. Ionic-liquid-based aqueous biphasic systems (IL-based ABS) have been raising significant interest as advantageous extraction and purification platforms; however, imidazolium-based ILs have been the primary option as phase-forming agents. Aiming the development of more sustainable IL-based ABS, in this work, six novel analogues of glycine-betaine ILs (AGB-ILs) were investigated. These ILs were synthesized and characterized in terms of purity, physico-chemical properties, ecotoxicity and ability to form ABS with tri-potassium citrate. The investigated AGB-ILs are composed of tri(*n*-alkyl[2-ethoxy-2-oxoethyl]ammonium/phosphonium and tri(*n*-alkyl[4-ethoxy-4-oxobutyl] ammonium/phosphonium cations with ethyl, *n*-propyl and *n*-butyl substituents, and the tosylate ([Tos]$^-$) anion. The synthesized ILs present degradation temperatures in the range from 220 to 265 °C, and are classified as relatively harmless regarding their ecotoxicity. The studied AGB-ILs display slightly lower thermal stability, but yet a lower ecotoxicity compared to the commercial IL 1-butyl-3-methylimidazolium tosylate. Their ability to form ABS was assessed, allowing to conclude that an expansion in the alkyl side chain length and spacer, as well as the presence of phosphonium instead of ammonium as central atom, increase the ability for phase separation in presence of tri-potassium phosphate aqueous solutions. The extraction performance of the studied AGB-ILs-based ABS was finally assessed with furfural, a platform chemical. In the majority of the studied systems, furfural preferentially migrates to the AGB-IL-rich phase, obtaining extraction efficiencies in a single step to the IL-rich phase up to 98%. These results reveal that novel ABS comprising AGB-ILs can be potentially used as separation platforms of bioactive compounds.

1. Introduction

Solvents display a significant role in the efficiency, cost and safety of most industrial processes (Welton, 2015); yet, aiming at more sustainable processes, the use of volatile organic solvents should be substantially reduced or even replaced by more sustainable alternatives (Erythropel et al., 2018). Triggered by the growing consciousness of population and regulation on current environmental problems, the pursuit for more benign solvents for reaction, extraction and separation processes has raised attention in the past years

* Corresponding author.
** Corresponding author.
E-mail addresses: maragfreire@ua.pt (M.G. Freire), aminou.mohamadou@univ-reims.fr (A. Mohamadou).

https://doi.org/10.1016/j.scp.2023.101132
Received 28 February 2023; Received in revised form 2 May 2023; Accepted 18 May 2023
Available online 4 July 2023

(Bogel-Lukasik, 2015). In this field, ionic liquids (ILs) and their respective aqueous solutions have shown to play a relevant role (Bogel-Lukasik, 2015; Ventura et al., 2017; Passos et al., 2014). Among these, aqueous solutions of ILs allow to decrease the solvent consumption, bringing environmental and economic benefits. The use of aqueous solutions of ILs also allows the reduction of energy inputs and the overall viscosity of systems, while improving the mass transfer and the efficiency and selectivity of extraction processes (Ventura et al., 2017). Furthermore, aqueous solutions of ILs allow the increased solubility of a myriad of natural compounds when compared with their solubility in the correspondent pure ILs (Ventura et al., 2017; Passos et al., 2014; de Faria et al., 2017; Sintra et al., 2018). As such, whenever possible, the use of aqueous solutions of ILs is advisable.

ILs, if properly designed, display some advantageous properties compared to conventional organic solvents, namely their negligible vapour pressure at room conditions, high thermal stability and high ionic conductivity (Freire et al., 2012a); yet, some of them also exhibit low biodegradability and high toxicity (Phuong et al., 2010). The majority of the studies resorting to ILs for the extraction of bioactive compounds focus on imidazolium-based ILs (Passos et al., 2014), which may present some undesirable issues. Aiming at moving towards more sustainable solvents, a series of bio-based ILs with a more benign character has been synthesized and applied (Marra et al., 2011; Hawatulaila et al., 2016; Pereira et al., 2018; Gaetano et al., 2015a; Ferreira et al., 2017a; Ren et al., 2016; An et al., 2015). In this field, cholinium-based ILs have been studied in extraction processes (Petkovic et al., 2010; Shahriari et al., 2013) and in the pretreatment of biomass (Ren et al., 2016; An et al., 2015; Hou et al., 2017). Carbohydrate- (Marra et al., 2011) and amino-acid-based (Hawatulaila et al., 2016) ILs have been designed to enhance their biocompatible character. Furthermore, ILs derived from glycine-betaine and their analogues (AGB-ILs) have shown to be promising extraction solvents of added-value compounds from biomass (Ferreira et al., 2017b). AGB-ILs are relevant solvent alternatives since glycine-betaine is an amino acid and abundant low cost zwitterionic compound. After the saccharose extraction step, this amino acid can be naturally found in sugar beet molasses (up to 27 wt%) (Gérardin et al., 2013). Nowadays, glycine-betaine, as well as their derivatives, are widely applied in cosmetic formulations and food supplements (Ferreira et al., 2017a). Albeit their high potential and benign characteristics (Ferreira et al., 2017a), AGB-ILs are still underexplored (Pereira et al., 2018, 2019; Gaetano et al., 2015a; Parajó et al., 2019; Goursaud et al., 2008; Capela et al., 2019). In particular, AGB-ILs have been applied in the extraction of pesticides from wastewater (Gaetano et al., 2015b) and metals from aqueous solutions (Messadi et al., 2013a; Zhou et al., 2015; Boudesocque et al., 2014).

Due to the potential interest of AGB-ILs, namely for the extraction of bioactive compounds from biomass and their separation, herein we report the synthesis and characterization of six new AGB-ILs comprising the tosylate anion ($[Tos]^-$). Their complete names, abbreviations and chemical structures are provided in Fig. 1. The series is mainly composed of ammonium-based AGB-ILs, with one phosphonium-based AGB-IL for comparison purposes. This way, it is possible to infer the central atom impact on the several properties addressed. *p*-toluenesulfonic acid has raised attention in the biomass pretreatment and fractionation (Li et al., 2020; Wang et al., 2020a, 2020b; Yang et al., 2019). Therefore, we investigated a series of AGB-ILs paired with the tosylate anion. The novel AGB-ILs were synthesized and characterized in terms of purity, thermal properties (decomposition temperature) and ecotoxicity against *Aliivibrio fischeri* (Steinberg et al., 1995). Ultimately, while foreseeing their application in separation processes in the biorefinery field, their ability to form aqueous biphasic systems (ABS) in presence of tri-potassium citrate was investigated. These systems were then evaluated in what concerns their extraction performance for furfural. Furfural is a relevant molecule within the biorefinery concept. It is currently considered a platform chemical for the sustainable production of chemicals and fuels (Jaswal et al., 2022).

2. Experimental section

2.1. Materials

Para-toluenesulfonic acid monohydrate (purity 99%) and silver nitrate (purity 99,5%) were acquired from Acros Organics. Tri(*n*-alkyl)[2(or 4)-ethoxy-2-oxoethyl(or 4-oxobutyl)ammonium/phosphonium bromide ($[R_3NC_2]Br$ or $[R_3NC_4]Br$ with R = ethyl, *n*-propyl or *n*-butyl, and $[Bu_3PC_2]Br$ were obtained by the method described in the literature (Pereira et al., 2019). Silver tosylate (AgTos) was synthesized by mixing an equimolar solution of *p*-toluenesulfonic acid and silver nitrate. Tri-potassium citrate monohydrate ($C_6H_5K_3O_7.H_2O$) (purity 99%) was acquired from Acros Organics. 1-Butyl-3-methylimidazolium tosylate ($[C_4C_1im][Tos]$) (purity 98%) was acquired from Iolitec. Furfural (purity 99%) was acquired from Sigma-Aldrich.

2.2. Synthesis of AGB-ILs

AGB-ILs were synthesized and dried under vacuum for at least 72 h at 45 °C, according to previous protocols reported in the literature (Gaetano et al., 2015a; Pereira et al., 2019; Messadi et al., 2013b). Their chemical structures are provided in Fig. 1. In particular, the AGB-ILs *N,N,N*-tri(ethyl)(2-ethoxy-2-oxoethyl)-1-ammonium tosylate ($[EtNC_2][Tos]$), *N,N,N*-tri(ethyl)(4-ethoxy-4-oxobutyl)-1-ammonium tosylate ($[EtNC_4][Tos]$), *N,N,N*-tri(*n*-propyl)(2-ethoxy-2-oxoethyl)-1-ammonium tosylate ($[PrNC_2][Tos]$), *N,N,N*-tri(*n*-propyl)(4-ethoxy-4-oxobutyl)-1-ammonium tosylate ($[PrNC_4][Tos]$), *N,N,N*-tri(*n*-butyl)(2-ethoxy-2-oxoethyl)-1-ammonium tosylate ($[BuNC_2][Tos]$) and tri(*n*-butyl)[2-ethoxy-2-oxoethyl]phosphonium tosylate ($[BuPC_2][Tos]$) were synthesized by the reaction of ethyl-2-bromoacetate and tri(*n*-alkyl)amine/phosphine (tri(*n*-alkyl)amine/phosphine = triethylamine, with tri(*n*-propyl)amine, tri(*n*-butyl)amine and tri(*n*-butyl)phosphine) by the method described earlier (Pereira et al., 2019), followed by the anionic metathesis reaction of the bromide by tosylate using siver tosylate. All these novel ILs are solid at room temperature and water-soluble. The elemental analysis of all synthesized AGB-ILs was performed using a PerkinElmer 2400C, H and N element analyzer, whose results are presented in Table 1. ^1H and ^{13}C nuclear magnetic resonance (NMR) was carried out to assess the purity of each AGB-IL, presenting a purity higher than 98%. The NMR assays were carried out at room temperature, using DMSO-d_6 as solvent, with a Bruker Advanced 1 spectrometer (300 MHz). The NMR spectra were recorded considering solvent signal (2.50 and 39.52ppm), and their chemical shift (δ) are expressed in ppm. The correspondent NMR spectra of each AGB-IL are given in the Supporting Information (Figs. S1 to S12).

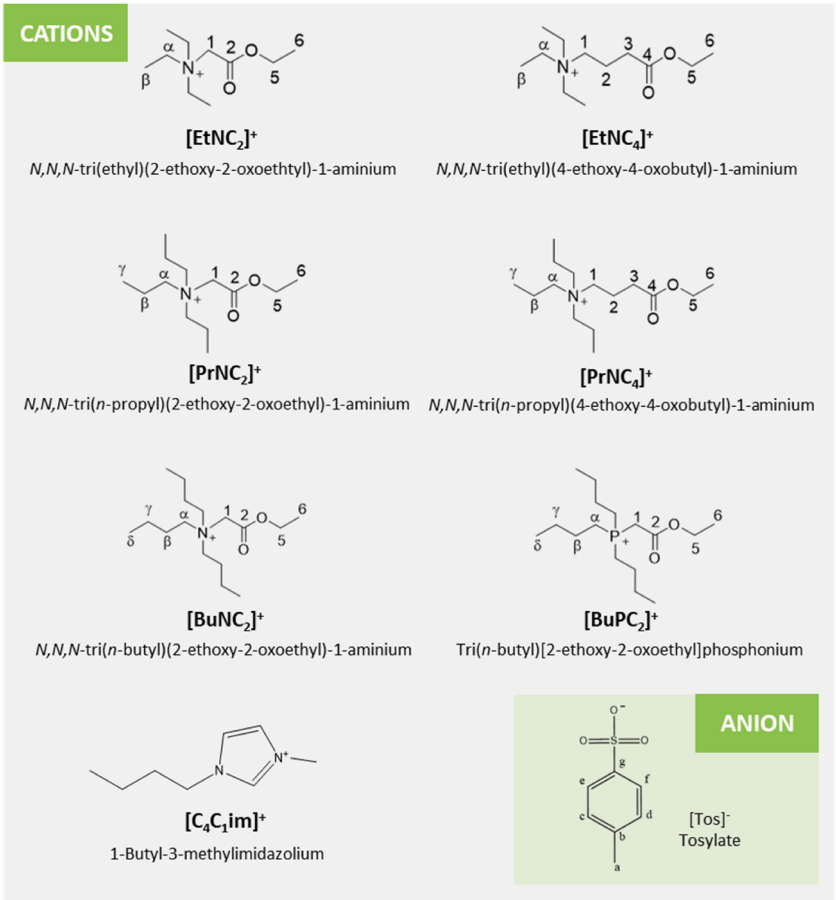

Fig. 1. Chemical structure, chemical name and abbreviation of the synthesized AGB-ILs and the commercial IL ([C_4C_1im][Tos]).

The peaks assignment is according to the atoms identified in Fig. 1. The respective characterization is given in Table 2. AGB-ILs samples were dried under vacuum for at least 48 h at room temperature before NMR and elemental analysis. The water content of the dried AGB-ILs was determined by Karl Fischer coulometry using a Metrohm 787 KF Titrino coulometer with Hydranal 34805 and Hydranal 37817 (from Fluka) as titrant.

Tri(*n*-alkyl)[2(or 4)-ethoxy-2-oxoethyl(or 4-oxobutyl)ammonium/phosphonium bromide (65 mmol) in 100 mL of a water-ethanol solution (v/v, 1/1) was added in slight excess to freshly prepared silver tosylate (19,53 g, 70 mmol), and gently heated (30–40 °C) for 1 h whilst stirring. The mixture was then stirred at room temperature for a night. The solid precipitate (AgBr and excess of AgTos) was filtered off, and the solvent was removed by rotary evaporation. The resultant sample was dissolved in dichloromethane (50 mL) to precipitate remaining silver tosylate, which was filtered off, and the filtrate evaporated to dryness. The resultant sample was dissolved in 50 mL of dichloromethane and washed with pure water several times until no residual bromide was detected with the use of $AgNO_3$ test of the aqueous phase. Then, the organic phase was evaporated and the obtained oily compound was dried under vacuum.

2.3. Decomposition temperature and ecotoxicity assessment

The decomposition temperature of the new AGB-ILs was determined according to the literature (Cardoso et al., 2021a). The responses were analysed with the Microtox® Omni™ Software (Volpi et al., 2009; Francisca et al., 2014).

2.4. Aqueous biphasic systems phase diagrams

Aqueous solutions of AGB-ILs ([$BuPC_2$][Tos], [$BuNC_2$][Tos], [$PrNC_4$][Tos], [$PrNC_2$][Tos], [$EtNC_4$][Tos], [$EtNC_2$][Tos]) and [C_4C_1im][Tos] at concentrations of 80 wt% and aqueous solutions of $C_6H_5K_3O_7.H_2O$ at 50 wt%, were prepared and used for the determination of the respective liquid-liquid phase diagrams and binodal curves. The salt ($C_6H_5K_3O_7.H_2O$) was chosen since citrate-based salts are biodegradable, non-toxic, and widely used as more sustainable alternatives in biological processes (Passos et al., 2012). Further details regarding the cloud point titration method are described in the Supporting Information and in the literature (Merchuk et al., 1998; Sintra et al., 2014).

Table 1
– Elemental analysis results (in weight percentage) of the synthesized AGB-ILs.

AGB-ILs	Molecular formula	MW ($g.mol^{-1}$)	Elemental analysis	
			Theorical	Obtained
$[EtNC_2][Tos]$ $\cdot 0.7H_2O$	$C_{17}H_{33.4}NO_{5.7}S$	372.09	C – 54.88% H – 8.23% N – 3.76% S – 8.62%	C – 54.93% H – 8.21% N – 4.14% S – 8.01%
$[EtNC_4][Tos]$ $\cdot 0.5H_2O$	$C_{19}H_{34}NO_{5.5}S$	396.54	C – 57.55% H – 8.64% N – 3.53% S – 8.08%	C – 57.12% H – 8.27% N – 3.73% S – 7.16%
$[PrNC_2][Tos]$ $\cdot 0.8H_2O$	$C_{20}H_{37}NO_6S$	419.57	C – 57.25% H – 8.89% N – 3.34% S – 7.64%	C – 57.41% H – 8.61% N – 3.64% S – 6.48%
$[PrNC_4][Tos]$ $\cdot 1.3H_2O$	$C_{22}H_{41.6}NO_{6.3}S$	453.03	C – 58.33% H – 9.26% N – 3.09% S – 7.08%	C – 58.58% H – 9.07% N – 3.58% S – 6.88%
$[BuNC_2][Tos]$ $\cdot 0.5H_2O$	$C_{23}H_{42}NO_{5.5}S$	452.65	C – 61.03% H – 9.35% N – 3.09% S – 7.08%	C – 61.40% H – 9.45% N – 3.52% S – 6.27%
$[BuPC_2][Tos]$ $\cdot 2H_2O$	$C_{23}H_{45}O_7PS$	496.64	C – 55.62% H – 9.13% S – 6.46%	C – 55.99% H – 8.98% S – 6.18%

2.5. Extraction of furfural

The compositions of the ternary mixtures (AGB-ILs + water + tri-potassium citrate) applied in the extraction experiments were selected according to the phase diagrams obtained in the present work, considering compositions that allow the formation of biphasic systems. An aqueous solution of furfural was prepared at a concentration of 12 $g.L^{-1}$, and used as the aqueous media to prepare each ABS. Each system was stirred and centrifuged for 15 min at 3000 rpm. Then, the system was left at room temperature for more 15 min to ensure equilibrium. Through a previous kinetic study, it was found that the equilibrium is attained after 15 min of centrifugation at 3000 rpm, for a total mass of the ABS of ca. 1 g. Furthermore, a cautious phase separation was accomplished and the amount of furfural in the top and bottom phase was quantified by high performance liquid chromatography (HPLC) with a diode-array detection (DAD).

Samples of each phase were filtered with a 0.20 μm syringe filter and furfural quantified by HPLC-DAD (Shimadzu, model PROMINENCE). HPLC analysis were performed with an analytical C18 reversed-phase column (250 × 4.60 mm), Kinetex 5 μm C18 100 Å, from Phenomenex. The mobile phase used consisted of 20% (v/v) of methanol and 80% (v/v) of ultra-pure water. The separation was conducted in isocratic mode, at a flow rate of 0.8 mL min^{-1} and using an injection volume of 10 μL. The column oven and the autosampler were operated at controlled temperature (35 °C). The wavelength was set at 268 nm and each sample was analysed at least in duplicate. Calibration curves were established with pure furfural dissolved in water.

3. Results and discussion

3.1. AGB-ILs characterization

Table 3 provides the AGB-ILs decomposition temperature (T_{dec}) corresponding to a weight loss of 10%, ranging between 220 and 266 °C. The thermal degradation temperature (T_{dec}) profile of all these AGB-ILs is provided in Figure S13 in the Supporting Information. The ILs thermal stabilities increase in the order: $[BuNC_2][TOS] < [BuPC_2][Tos] < [PrNC_2][Tos] < [PrNC_4][Tos] < [EtNC_2][Tos] < [EtNC_4][Tos]$.

AGB-ILs comprising the bromide anion have an increase in their thermal stability with the increase of the alkyl chain length of the cation (Pereira et al., 2018). When compared with AGB-ILs with the same spacer size generated in this study and paired with the tosylate anion, the thermal stabilities increase in the opposite order, i.e. $[BuNC_2]^+ < [PrNC_2]^+ < [EtNC_2]^+$, meaning that the presence of a larger anion ($[Tos]^-$) reverses the thermal stability profile. Furthermore, surface-active analogues of glycine-betaine ILs (AGB-SAILs) sharing the same cations but combined with dodecylbenzenesulfonate ($[DBS]^-$) anion, reported in the literature (Cardoso et al., 2021a), have a different trend in the thermal stability when compared with the bromide and tosylate counterparts. This set of works (Pereira et al., 2019; Cardoso et al., 2021b) and the current one reveal that each AGB-IL series present a different thermal stability profile, emphasizing the relevance of the IL anion.

Amongst the ammonium-based cations, the maximum degradation temperature is reached with the IL comprising the *n*-ethyl groups. Furthermore, $[BuPC_2][Tos]$ is more thermally stable than $[BuNC_2][Tos]$, being in agreement with the literature (Cardoso et al., 2021b; Carvalho et al., 2014). In particular, by analysing a previously reported work (Cardoso et al., 2021a) comprising AGB-

Tables 2
–^{1}H and ^{13}C NMR peak assignments and synthesis yield of the synthesized AGB-ILs.

AGB-ILs	Yield	^{1}H NMR δ/ppm (300.13 MHz, DMSO-d_6)	^{13}C NMR δ/ppm (75.47 MHz, DMSO-d_6)
[$EtNC_2$][Tos]·0.7H_2O	20.16 g (85%)	1.11–1.30 [12H, m, CH_3(β,6)]; 2.28 [3H, s, CH_3(a)]; 3.47 [6H, quad, 7.3 Hz, CH_2(α)]; 4.21 [3H, quad, 7.1 Hz, CH_2(5)]; 4.33 [2H, s, CH_2(1)]; 7.12 [2H, m, CH(c,d)]; 7.49 [2H, m, CH(e,f)].	7.39 [CH_3(β)]; 13.74 [CH_3(6)]; 20.77 [CH_3(a)]; 53.93 [CH_2(α)]; 54.99 [CH_2(1)]; 62.00 [CH_2(5)]; 125.48 [CH(e,f)]; 128.06 [CH(c,d)]; 137.66 [C(b)]; 145.74 [C(g)]; 164.87 [C=O(2)].
[$EtNC_4$][Tos]·0.5H_2O	22.34 g (80%)	1.06–1.26 [12H, m, CH_3(β,6)]; 1.79 [2H, m, CH_2 (2)]; 2.28 [3H, s, CH_3 (a)]; 2.41 [2H, t, 6.8 Hz CH_2(3)]; 3.04–3.29 [8H, m, CH_2(α,1)]; 4.07 [2H, quad, 7.1 Hz, CH_2(5)]; 7.12 [2H, m, CH(c,d)]; 7.50 [2H, m, CH(e,f)].	7.04 [CH_3(β)]; 14.08 [CH_3(6)]; 16.65 [CH_2(2)]; 20.77 [CH_3(a)]; 29.71 [CH_2(3)]; 52.02 [CH_2(α)]; 54.95 [CH_2(1)]; 60.20 [CH_2(5)]; 125.51 [CH(e,f)]; 128.09 [CH(c,d)]; 137.70 [C(b)]; 145.74 [C(g)]; 172.06 [C=O(4)].
[$PrNC_2$][Tos]·0.8H_2O	24.31 g (81%)	0.86 [9H, t, 7.2 Hz, CH_3(γ)]; 1.23 [3H, t, 7.1 Hz, CH_3(6)]; 1.64 [6H, m, CH_2(β)]; 2.28 [2.4H, s, CH_3 (a)]; 3.38 [6H, m, CH_2(α)]; 4.22 [2H, quad, 7.1 Hz, CH_2(5)]; 4.38 [2H, s, CH_2(1)]; 7.11 [1.6H, m, CH(c,d)]; 7.48 [1.6H, m, CH(e,f)].	13.75 [CH3(6)]; 15.07 [CH2(β)]; 20.76 [CH3(a)]; 56.56 [CH2(1)]; 61.01 [CH2(α)]; 62.03 [CH2(5)]; 125.48 [CH(e,f)]; 128.03 [CH(c,d)]; 137.60 [C(b)]; 145.76 [C(g)]; 164.84 [C=O(2)].
[$PrNC_4$][Tos]·1.3H_2O	24.87 g (81%)	0.89 [9H, t, 7.2 Hz, CH_3(γ)]; 1.20 [3H, t, 7.1 Hz, CH_3(6)]; 1.62 [8H, m, CH_2(β)]; 1,80 [2H, m, CH_2(2)]; 2.41 [2H, t, 6.8 Hz CH_2(3)]; 2.28 [3H, s, CH_3(a)]; 3.04–3,21 [8H, m, CH_2(α,1)]; 4.07 [2H, quad, 7.1 Hz, CH_2(5)]; 7.13 [2H, d, CH(c,d)]; 7.48 [2H, d, CH(e,f)].	10.87 [CH_3(γ)]; 14.40 [CH_3(6)]; 15.17 [CH_2(β)]; 17.46 [CH_3(2)]; 21.29 [CH_2(a)]; 30.12 [CH_2(3)]; 57.03 [CH_2(1)]; 59.56 [CH_2(α)]; 60.62 [CH_2(5)]; 126.02 [CH(c,d)]; 128.56 [CH(e,f)]; 137.98 [C(b)]; 146.10 [C(g)]; 174.24 [C=O(4)].
[$BuNC_2$][Tos]·0.5H_2O	24.61 g (82%)	0.90 [9H, t,7.3 Hz, CH_3(δ)]; 1.15–1.39 [9H,m,CH_2(γ)+ CH_3 (6)]; 1.60 [6H, m, CH_2(β)]; 2.28 [3H, s, CH3 (a)]; 3.42 [6H, m, CH_2(α)]; 4.21 [2H, quad, 7.1 Hz, CH_2(5)]; 4.39 [2H, s, CH_2(1)]; 7.11 [2H, m, CH(c,d)]; 7.50 [2H, m, CH(e,f)].	13.37 [CH_3(δ)]; 13.71 [CH_3(6)]; 19.08 [CH_2(γ)]; 20.73 [CH_3(a)]; 23.27 [CH_2(β)]; 56.46 [CH_2(1)]; 59.31 [CH_2(α)]; 61.97 [CH_2(5)]; 125.47 [CH(e,f)]; 127.97 [CH(c,d)]; 137.75 [C(b)]; 145.78 [C(g)].
[$BuPC_2$][Tos]·2H_2O	25.03 g (80%)	0.89 [9H, t, 7.1 Hz CH_3(δ)]; 1.22 [3H, t, 7.1 Hz, CH_3(6)]; 1.42 [12H, m, CH_2(β, γ)]; 2.29 [9H, m, CH_3(a), CH_2(α)]; 3.81 [2H, d, 14.5 Hz, CH_2(1)]; 4.17 [2H, quad, 7.1 Hz, CH_2(5)]; 7.11 [2H, m, CH(c,d)]; 7.49 [2H, m, CH(e,f)].	13.19 [CH_3(δ)]; 13.77 [CH_3(6)]; 18.14 [d, 47.3 Hz, CH_2(α)]; 20.74 [CH_3(a)]; 22.58 [d, 4.5 Hz, CH_2(γ)]; 23.27 [d, 16.5 Hz, CH_2(β)]; 25.52 [d, 48.7 Hz, CH_2(1)]; 62.04 [CH_2(5)]; 125.46 [CH(e,f)]; 128.00 [CH(c,d)]; 137.61 [C(b)]; 145.73 [C(g)]; 165.46 [d,4.4 Hz,C=O(2)].

Table 3
Decomposition (T_{dec}) temperatures for the synthesized AGB-ILs.

AGB-ILs	T_{dec} (°C)
[$EtNC_2$][Tos]	237.1
[$EtNC_4$][Tos]	264.6
[$PrNC_2$][Tos]	230.5
[$PrNC_4$][Tos]	236.4
[$BuNC_2$][Tos]	220.2
[$BuPC_2$][Tos]	221.3
[C_4C_1im][Tos]	372.0 (Cao and Mu, 2014)

SAILs sharing the same cations, it is shown that the [$BuPC_2$][Tos] is more thermally stable than [$BuNC_2$][Tos]. Tsunashima et al. (2010) attributed this trend to the existence of empty *d*-orbitals on the phosphorus atom, enhancing the phosphorus reactivity.

Regarding the SAILs containing ammonium and phosphonium cations with equivalent alkyl chains, namely [$PrNC_2$][Tos] and [$PrNC_4$][Tos] versus [$EtNC_2$][Tos] and [$EtNC_4$][Tos], the most stable AGB-IL is the one that holds longer spacers. These results are in agreement with the results reported in literature (Gaetano et al., 2015a; Cardoso et al., 2021b). Gaetano et al. (2015a) stated that the degradation temperature rises with a higher number of carbon atoms in alkyl groups comprised on glycine-betaine ILs. Finally, when comparing the AGB-ILs with the [Tos]$^-$ anion with the commercially available IL ([C_4C_1im][Tos]), the latter one is more thermally stable, which is a result of the imidazolium cation instead of a quaternary ammonium one.

The performance of chemical industrial processes heavily depends on the cost and environmental impact of the applied solvents. In this sense, it is mandatory to reduce the environmental impact resulting from the use of solvents in chemical processes, evaluating their toxicity to foresee their potential use in industrial plants (Phuong et al., 2010; Capello et al., 2007). Microtox® assays were applied in this work to estimate the impact of all novel AGB-ILs against the marine luminescent bacteria *A. fischeri*, being the correspondent EC_{50} values depicted in Fig. 2. It was applied an exposure time of 30 min to ensure the enough exposure to the AGB-ILs aqueous solutions (Volpi et al., 2009; Francisca et al., 2014). In Fig. 2 it is compared the EC_{50} data of the novel AGB-ILs with the sodium tosylate salt and a commercial IL ([C_4C_1im][Tos]). Considering the Passino and Smith hazard ranking (Passino and Smith, 1987), all the novel AGB-ILs can be considered as relatively harmless (at 30 min of exposure with an EC_{50} higher than 1000 mg.L^{-1}), which is the best toxicity level in the ranking. By definition, the higher the EC_{50} values, the less toxic is the target compound. Remarkably, all of the AGB-ILs here studied display a lower toxicity to *A. fischeri* than the commercial salt available (sodium tosylate) and the commercial imidazolium-based counterpart ([C_4C_1im][Tos]) (Ventura et al., 2012), being considered excellent alternatives to be applied in large-scale processes in terms of toxicity and environmental risk.

Since all AGB-ILs share the same anion, the identified ecotoxicity values are a result of the IL cation. The AGB-ILs' toxicity towards the bacteria increase according to the following cation rank: $[BuPC_2]^+ < [BuNC_2]^+ < [PrNC_4]^+ < [PrNC_2]^+ < [EtNC_4]^+ \approx [EtNC_2]^+$. [$EtNC_2$][Tos] and [$EtNC_4$][Tos] are the most toxic AGB-ILs, while the [$BuPC_2$][Tos] is the less toxic, which is unexpected considering previous studies showing that the increase of the cation alkyl chain length promotes a higher ecotoxicity (Ventura et al., 2012; Romero et al., 2008; Couling et al., 2006). However, these results corroborate previously reported results obtained with surface-active AGB-ILs (Cardoso et al., 2021b). The opposite ecotoxicity trend observed seems to be an inherent characteristic of AGB-ILs. Parajó et al. (2019) established that the spacer in the cation of the AGB-IL displays a significant influence in the toxicity of the IL, corroborating the obtained results when comparing the following cation pairs: $[EtNC_2]^+/[EtNC_4]^+$ and $[PrNC_2]^+/[PrNC_4]^+$. ILs with a longer spacer in the cation are less toxic. When comparing the ILs with cations with different central atoms (N vs. P), it is shown that the phosphonium-based IL is less toxic than its ammonium-based counterpart. This trend is in good agreement with the literature (Pereira et al., 2018; Couling et al., 2006). Moreover, given the fact that [C_4C_1im][Tos] displays an imidazolium structure, it is expected that this configuration leads to a more toxic IL than their linear-based counterparts with the same number of carbon atoms in the aliphatic chains attached to the N central atom ([$EtNC_4$][Tos] and [$PrNC_4$][Tos]). This hyphotesis is indeed confirmed with the obtained data.

3.2. Phase diagrams and extraction of furfural

Aiming at exploring the use of the novel AGB-ILs in liquid-liquid separation processes, their potential to form ABS with salts was addressed. The ternary phase diagrams of the six AGB-ILs ([$BuPC_2$][Tos], [$BuNC_2$][Tos], [$PrNC_4$][Tos], [$PrNC_2$][Tos], [$EtNC_4$][Tos] and [$EtNC_2$][Tos]) + $C_6H_5K_3O_7.H_2O$ + water were determined at atmospheric pressure, 25 °C and pH 8.0–8.5. The correspondent phase diagrams are presented in Fig. 3. Further details regarding the binodal curves and the correspondent constants are given in the Supporting Information (Tables S1 to S8). All the experimental data of the binodal curves were fitted using one of the most adequate equations to correlate IL-based ABS experimental data (Freire et al., 2012a). The corresponding regression parameters and correlation coefficients (R^2) are given in the Supporting Information (Table S8).

In all ABS, the top phase is the AGB-IL-rich phase, and the bottom phase is mainly composed of $C_6H_5K_3O_7.H_2O$ and water. By definition, in the phase diagrams, the monophasic and biphasic regions are placed below and above each solubility curve, respectively

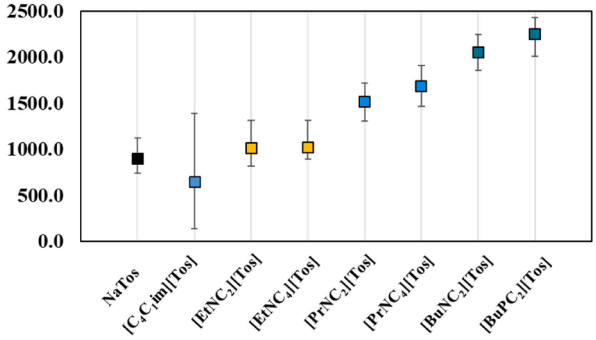

Fig. 2. Microtox® EC_{50} values (mg.L^{-1}) for *Aliivibrio fischeri* after 30 min of exposure time to aqueous solutions of AGB-ILs, sodium tosylate and [C_4C_1im][Tos] (the latter one taken from Ventura et al. (Ventura et al., 2012), corresponds to a 15 min of exposure time).

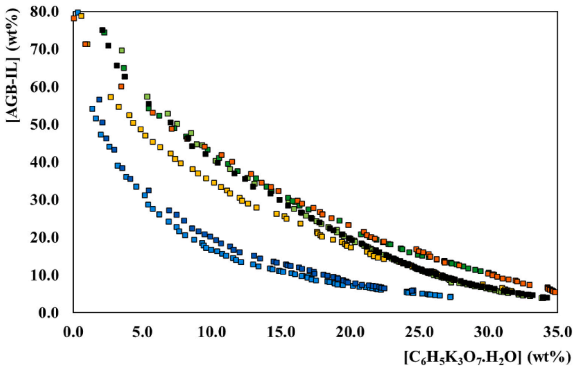

Fig. 3. - Phase diagrams of the systems composed of AGB-IL + $C_6H_5K_3O_7.H_2O$ + H_2O at 25 °C: (■) [$EtNC_2$][Tos]; (■) [$EtNC_4$][Tos]; (■) [$PrNC_2$][Tos]; (■) [$PrNC_4$][Tos]; (■) [$BuNC_2$][Tos]; (■) [$BuPC_2$][Tos]; (■) [C_4C_1im][Tos].

(Freire et al., 2012b). Phase diagrams with a smaller area below the solubility curve display a higher ability to form an ABS, thus requiring a lower amount of IL or salt to form two phases. Globally, the capacity of AGB-ILs to form ABS at 25 °C, at 15 wt% of $C_6H_5K_3O_7.H_2O$, increases in the following order: [$PrNC_4$][Tos] ≈ [$EtNC_4$][Tos] ≈ [$EtNC_2$][Tos] ≈ [C_4C_1im][Tos] < [$PrNC_2$][Tos] < [$BuNC_2$][Tos] < [$BuPC_2$][Tos]. Since all studied compounds comprise the tosylate anion ($[Tos]^-$), the differences verified amongst these ILs is a direct impact of the IL cation nature. It is expected that ILs comprising longer alkyl side chains are more hydrophobic, and thus, more able to be salted-out from aqueous solutions (Pereira et al., 2018; Sintra et al., 2014; Belchior et al., 2020; E Silva et al., 2014). In this sense, the [$BuPC_2$][Tos] and [$BuNC_2$][Tos] demand a lower amount of salt to form an ABS, as obtained in the current work and being in agreement with the literature (Pereira et al., 2018; Sintra et al., 2014; Belchior et al., 2020; E Silva et al., 2014). The phosphonium-based AGB-IL allow an easier phase separation to form ABS comparing to its ammonium counterpart, mostly due to the cation central atom charge distribution that increases the IL hydrophobic character, as reported in the literature (Carvalho et al., 2014).

The fact that the less toxic AGB-IL ([$BuPC_2$][Tos]) presents a higher ability to create ABS with $C_6H_5K_3O_7.H_2O$ is an important advantage when foreseeing its application as extraction and purification platforms, since a higher amount of water will be introduced in the system. This allows to reduce the overall environmental impact of the process.

In order to evaluate the potential of the AGB-ILs-based ABS to be applied as separation platforms, it was selected a fixed mixture point (≈25 wt% of IL + 25 wt% of $C_6H_5K_3O_7.H_2O$) in the biphasic region and the extraction efficiency of furfural was investigated at 25 °C. The extraction efficiency results are provided in Fig. 4. The furfural content was quantified through HPLC-DAD, at a wavelength of 268 nm, using a calibration curve previously determined. The percentage extraction efficiencies of furfural ($EE_{furfural}$%)), defined as the percentage ratio between the amount of furfural in the IL-rich phase (top phase) and that in the total mixture, was determined according to Eq. (1):

$$EE_{furfural}\,(\%) = \frac{w_{furfural}^{top\ phase}}{w_{furfural}^{top\ phase} + w_{furfural}^{bottom\ phase}} \quad (1)$$

where $w_{furfural}^{top\ phase}$ and $w_{furfural}^{bottom\ phase}$ are the weight of furfural present in the top (IL-rich phase) and in the salt-rich phase (bottom phase) aqueous phases, respectively.

In all ABS systems, furfural preferentially migrates to the IL-rich top phase, with extraction efficiencies up to 98%. This high single-step separation corroborates the contribution of the salt ($C_6H_5K_3O_7.H_2O$) as a strong salting-out agent. The extraction efficiency of furfural using these novel AGB-ILs as phase-forming components increases in the following order: [$EtNC_2$][Tos] < [$EtNC_4$]

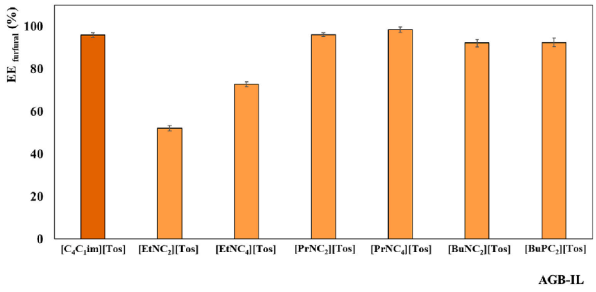

Fig. 4. Extraction efficiency of furfural ($EE_{furfural}$ (%)) of the AGB-IL-based ABS (≈25 wt% of IL + 25 wt% of $C_6H_5K_3O_7.H_2O$) at 25 °C to the IL-rich top phase.

[Tos] < [$BuNC_2$][Tos] ≈ [$BuPC_2$][Tos] ≈ [$PrNC_2$][Tos] ≈ [$PrNC_4$][Tos], leading to the conclusion that for the particular case of the recovery of furfural to the ABS top phase, the highest extraction efficiencies of furfural are obtained when using ILs with an intermediate hydrophobicity. This trend reveals that the partition of furfural depends on the contribution of different factors, namely the ability of the AGB-ILs and the salt to form ABS, the specific interactions established between the ILs and the target compound and the water content of the phases (Pereira et al., 2018, 2019). Regarding the AGB-ILs pair [$EtNC_2$][Tos]/[$EtNC_4$][Tos], it is possible to determine that the ones that display longer spacers are the ones that present higher extraction efficiencies of furfural. Concerning the phosphonium-based AGB-IL ([$BuPC_2$][Tos]) and its ammonium counterpart ([$BuNC_2$][Tos]), there is no difference in the extraction efficiency. Globally, most of the AGB-ILs here reported present a similar ability to recover furfural to the top phase, except for [$EtNC_2$][Tos] and [$EtNC_4$][Tos], comparing to the extraction performance of the commercially available IL ([C_4C_1im][Tos]).

The results here reported endorse the potential of AGB-IL-based ABS as extraction platforms and emphasizes the possibility of these novel ILs to replace the widely used imidazolium-based ILs (Ullah et al., 2018). Imidazolium-based ILs are largely involved in the furfural production processes, as solvents and/or catalysts (Pei et al., 2008); however, there is a lack of studies regarding the recovery of furfural applying liquid-liquid extraction processes. Pei et al. (2008) reported the use of fluorinated imidazolium-based ILs ([$C_nC_1$im][PF_6]) to recover about 73% of the total furfural to the IL-rich phase. This approach reports a lower extraction efficiency comparing to the one here reported using [$PrNC_4$][Tos] (98%). In addition, AGB-IL-based ABS decrease the overall toxicity of the process.

4. Conclusions

Aiming at the development of more biocompatible ABS to be applied in the extraction and separation of high-value compounds, a series of AGB-ILs was here synthesized and characterized. These ILs, based on analogues of glycine-betaine, were characterized by elemental analysis and NMR, decomposition temperature and ecotoxicity, and finally applied in the formation of ABS and extraction of furfural. A commercial imidazolium-based IL and a tosylate salt were also considered for comparison purposes.

Concerning the thermal stability, the novel AGB-ILs here reported display a T_{dec} between 220 and 260 °C. The novel AGB-ILs display a lower toxicity to *A. fischeri* than the commercial salt (sodium tosylate) and the imidazolium-based IL ([C_4C_1im][Tos]), being considered excellent alternatives to be applied in large-scale processes in terms of toxicity and environmental risk. However, further studies must be carried out to fully understand the toxicity mechanism behind these AGB-ILs. Aside from the negligible ecotoxicity of AGB-ILs, they also allow to create ABS with organic salts and provide high extraction efficiencies of furfural (up to 98%) to the top IL-rich phase. In particular, the most benign AGB-ILs display the higher ability to form an ABS, thus requiring a reduced amount of IL or salt to form two distinct phases, which is an advantage in scaled-up processes. It is expectable that the AGB-ILs here reported will have potential in the development of extraction and separation processes of other added-value bioactive compounds.

Author statement

Inês S. Cardoso: Investigation, Methodology, Writing - Original draft preparation;
Filipe H. B. Sosa: Investigation, Methodology, Writing - Reviewing and Editing.
Armando J. D. Silvestre: Supervision, Methodology, Writing - Reviewing and Editing.
Anthony Robert: Investigation, Methodology, Writing - Reviewing and Editing.
Mara G. Freire: Conceptualization, Methodology, Supervision, Writing - Reviewing and Editing, Funding acquisition, Project administration.
Aminou Mohamadou: Conceptualization, Methodology, Supervision, Writing - Reviewing and Editing, Funding acquisition, Project administration.

Declaration of competing interest

There are no conflicts of interest to declare.

Data availability

Data will be made available on request.

Acknowledgments

This work was developed within the scope of the project CICECO-Aveiro Institute of Materials, UIDB/50011/2020, UIDP/50011/2020 & LA/P/0006/2020, financed by national funds through the FCT/MEC (PIDDAC). Inês S. Cardoso acknowledges the PhD FCT grant SFRH/BD/139801/2018.

Appendix A. Supplementary data

Supplementary data to this article can be found online at https://doi.org/10.1016/j.scp.2023.101132.

References

An, Y.X., Zong, M.H., Wu, H., Li, N., 2015. Pretreatment of lignocellulosic biomass with renewable cholinium ionic liquids: biomass fractionation, enzymatic digestion and ionic liquid reuse. Bioresour. Technol. 192, 165–171.

Belchior, D.C.V., Quental, M.V., Pereira, M.M., Mendonça, C.M.N., Duarte, I.F., Freire, M.G., 2020. Performance of tetraalkylammonium-based ionic liquids as constituents of aqueous biphasic systems in the extraction of ovalbumin and lysozyme. Sep. Purif. Technol. 233, 116019.

Bogel-Lukasik, R., 2015. Ionic liquids in the biorefinery concept : challenges and perspectives. RSG Green Chemistry.

Boudesocque, S., Mohamadou, A., Dupont, L., 2014. Efficient extraction of gold from water by liquid-liquid extraction or precipitation using hydrophobic ionic liquids. New J. Chem. 38, 5573–5581.

Cao, Y., Mu, T., 2014. Comprehensive investigation on the thermal stability of 66 ionic liquids by thermogravimetric analysis. Ind. Eng. Chem. Res. 53, 8651–8664.

Capela, E.V., Santiago, A.E., Rufino, A.F.C.S., Tavares, A.P.M., Pereira, M.M., Mohamadou, A., Aires-Barros, R.M., Coutinho, J.A.P., Azevedo, A.M., Freire, M.G., 2019. Sustainable strategies based on glycine-betaine analogues ionic liquids for the recovery of monoclonal antibodies from cell culture supernatants. Green Chem. 21, 5671–5682.

Capello, C., Fischer, U., Hungerbu, K., 2007. What is a green solvent? A comprehensive framework for the environmental assessment of solvents. Green Chem. 9, 927–934.

Cardoso, I.S., de Faria, E.L.P., Silvestre, A.J.D., Freire, M.G., Mohamadou, A., 2021a. Synthesis and characterization of analogues of glycine-betaine surface-active ionic liquids. J. Mol. Liq. 342, 117440.

Cardoso, I.S., de Faria, E.L.P., Silvestre, A.J.D., Freire, M.G., Mohamadou, A., 2021b. Synthesis and characterization of analogues of glycine-betaine surface-active ionic liquids. J. Mol. Liq. 342.

Carvalho, P.J., Ventura, S.P.M., Batista, M.L.S., et al., 2014. Understanding the impact of the central atom on the ionic liquid behavior : phosphonium vs ammonium cations Understanding the impact of the central atom on the ionic liquid behavior : phosphonium vs ammonium cations. J. Chem. Phys. 140, 505–518.

Couling, D.J., Bernot, R.J., Docherty, K.M., Dixon, K., Maginn, E.J., 2006. Assessing the factors responsible for ionic liquid toxicity to aquatic organisms via quantitative structure – property relationship modeling. Green Chem. 8, 82–90.

de Faria, E.L.P., Shabudin, S.V., Claúdio, A.F.M., Válega, M., Domingues, F.M.J., Freire, C.S.R., Silvestre, A.J.D., Freire, M.G., 2017. Aqueous solutions of surface-active ionic liquids: remarkable alternative solvents to improve the solubility of triterpenic acids and their extraction from biomass. ACS Sustain. Chem. Eng. 5, 7344. –7351.

E Silva, F.A., Sintra, T., Ventura, S.P.M., Coutinho, J.A.P., 2014. Recovery of paracetamol from pharmaceutical wastes. Sep. Purif. Technol. 122, 315–322.

Erythropel, H.C., Zimmerman, J.B., de Winter, T.M., et al., 2018. The Green ChemisTREE: 20 years after taking root with the 12 principles. Green Chem. 20, 1919–1961.

Ferreira, A.M., Morais, E.S., Leite, A.C., Mohamadou, A., Holmbom, B., Holmbom, T., Neves, B.M., Coutinho, J.A.P., Freire, M.G., Silvestre, A.J.D., 2017a. Enhanced extraction and biological activity of 7- hydroxymatairesinol obtained from Norway spruce knots using aqueous solutions of ionic liquids. Green Chem. 19, 2626–2635.

Ferreira, A.M., Morais, E.S., Leite, A.C., Mohamadou, A., Holmbom, B., Holmbom, T., Neves, B.M., Coutinho, J.A.P., Freire, M.G., Silvestre, A.J.D., 2017b. Enhanced extraction and biological activity of 7-hydroxymatairesinol obtained from Norway spruce knots using aqueous solutions of ionic liquids. Green Chem. 19, 2626–2635.

Francisca, A., Siopa, F., Figueiredo, B.F.H.T., Gonçalves, A.M.M., Pereira, J.L., Gonçalves, F., Coutinho, J.A.P., Afonso, C.A.M., Ventura, S.P.M., 2014. Ecotoxicology and Environmental Safety Sustainable design for environment-friendly mono and dicationic cholinium-based ionic liquids. Ecotoxicol. Environ. Saf. 108, 302–310.

Freire, M.G., Cláudio, A.F.M., Araújo, J.M.M., Coutinho, J.A.P., Marrucho, I.M., Canongia Lopes, J.N., Rebelo, L.P.N., 2012a. Aqueous biphasic systems: a boost brought about by using ionic liquids. Chem. Soc. Rev. 41, 4966–4995.

Freire, M.G., Cláudio, A.F.M., Araújo, J.M.M., Coutinho, J.A.P., Marrucho, I.M., Lopes, J.N.C., Rebelo, L.P.N., 2012b. Aqueous biphasic systems: a boost brought about by using ionic liquids. Chem. Soc. Rev. 41, 4966.

Gaetano, Y De, Mohamadou, A., Boudesocque, S., Hubert, J., Plantier-royon, R., Dupont, L., 2015a. Ionic liquids derived from esters of Glycine Betaine : synthesis and characterization. J. Mol. Liq. 207, 60–66.

Gaetano, Y De, Hubert, J., Mohamadou, A., Boudesocque, S., Plantier-Royon, R., Renault, J.-H., Dupont, L., 2015b. Removal of pesticides from wastewater by ion pair centrifugal partition extraction using betaine-derived ionic liquids as extractants. Chem. Eng. J. 285, 596–604.

Gérardin, C., Rebout, J., Bonne, M., Lebeau, B., 2013. Ecodesign of ordered mesoporous silica materials. Chem. Soc. Rev. 42, 4217–4255.

Goursaud, F., Berchel, M., Legros, N., 2008. Glycine betaine as a renewable raw material to “ greener ” new cationic surfactants. Green Chem. 3, 310–320.

Hawatulaila, S., Adawiyah, N., Aini, A., 2016. Ecotoxicity study of amino acid ionic liquids towards Danio rerio fish : effect of cations. Procedia Eng. 148, 401–408.

Hou, Q., Ju, M., Li, W., Chen, Y., Yang, Q., 2017. Pretreatment of lignocellulosic biomass with ionic liquids and ionic liquid-based solvent systems. Molecules 22, 1–24.

Jaswal, A., Singh, P.P., Mondal, T., 2022. Furfural-a versatile, biomass-derived platform chemical for the production of renewable chemicals. Green Chem. 24, 510–551.

Li, P., Ji, H., Shan, L., Dong, Y., Long, Z., Zou, Z., Pang, Z., 2020. Insights into delignification behavior using aqueous p-toluenesulfonic acid treatment: comparison with different biomass species. Cellulose 27, 10345–10358.

Marra, A., Chiappe, C., Mele, A., 2011. Sugar-derived ionic liquids. Chimia 65, 76–80.

Messadi, A., Mohamadou, A., Boudesocque, S., Dupont, L., Guillon, E., 2013a. Task-specific ionic liquid with coordinating anion for heavy metal ion extraction: cation exchange versus ion-pair extraction. Sep. Purif. Technol. 107, 172–178.

Merchuk, J.C., Andrews, B.A., Asenjo, J.A., 1998. Aqueous two-phase systems for protein separation Studies on phase inversion. J. Chromatogr. B 711, 285–293.

Messadi, A., Mohamadou, A., Boudesocque, S., Dupont, L., Fricoteaux, P., Nguyen-van-nhien, A., Courty, M., 2013b. Syntheses and characterisation of hydrophobic ionic liquids containing trialkyl (2-ethoxy-2-oxoethyl) ammonium or N- (1-methylpyrrolidyl-2-ethoxy-2-oxoethyl) ammonium cations. J. Mol. Liq. 184, 68–72.

Parajó, J.J., Macário, I.P.E., De Gaetano, Y., Dupont, L., Salgado, J., Pereira, J.L., Gonçalves, F.J.M., Mohamadou, A., Ventura, S.P.M., 2019. Glycine-betaine-derived ionic liquids: synthesis, characterization and ecotoxicological evaluation. Ecotoxicol. Environ. Saf. 184, 109580.

Passino, R.M.A.Y., Smith, B., 1987. Acute bioassays and hazard evaluation of representative contaminants detected in great lakes fish. Environ. Toxicol. Chem. 6, 901–907.

Passos, H., Ferreira, A.R., Cláudio, A.F.M., Coutinho, J.A.P., Freire, M.G., 2012. Characterization of aqueous biphasic systems composed of ionic liquids and a citrate-based biodegradable salt. Biochem. Eng. J. 67, 68–76.

Passos, H., Freire, M.G., Coutinho, J.A.P., 2014. Ionic liquids solutions as extractive solvents of value-added compounds from biomass. Green Chem. 16, 4786–4815.

Pei, Y., Wu, K., Wang, J., Fan, J., 2008. Recovery of furfural from aqueous solution by ionic liquid based liquid-liquid extraction. Separ. Sci. Technol. 43, 2090–2102.

Pereira, M.M., Almeida, M.R., Gomes, J., Rufino, A.F.C.S., Rosa, M.E., Coutinho, J.A.P., Mohamadou, A., Freire, M.G., 2018. Glycine-betaine ionic liquid analogues as novel phase-forming components of aqueous biphasic systems. Biotechnol. Prog. 34, 1205–1212.

Pereira, M.M., Pedro, S.N., Gomes, J., Sintra, T.E., Ventura, S.P.M., Coutinho, J.A.P., Freire, M.G., Mohamadou, A., 2019. Synthesis and characterization of analogues of glycine-betaine ionic liquids and their use in the formation of aqueous biphasic systems. Fluid Phase Equil. 494, 239–245.

Petkovic, M., Ferguson, J.L., Gunaratne, H.Q.N., Ferreira, R., Leit, M.C., Seddon, K.R., Rebelo, N., Silva, C., 2010. Novel biocompatible cholinium-based ionic liquids — toxicity and biodegradability. Green Chem. 12, 643–649.

Phuong, T., Pham, T., Cho, C., Yun, Y., 2010. Environmental fate and toxicity of ionic liquids : a review. Water Res. 44, 352–372.

Ren, H., Zong, M.-H., Wu, H., Li, N., 2016. Efficient pretreatment of wheat straw using novel renewable cholinium ionic liquids to improve enzymatic saccharification. Ind. Eng. Chem. Res. 55, 1788–1795.

Romero, A., Santos, A., Tojo, J., Rodríguez, A., 2008. Toxicity and biodegradability of imidazolium ionic liquids. J. Hazard Mater. 151, 268–273.

Shahriari, S., Tomé, L.C., Araújo, J.M.M., Rebelo, L.P.N., Coutinho, J.A.P., Marrucho, I.M., Freire, M.G., 2013. Aqueous biphasic systems: a benign route using cholinium-based ionic liquids. RSC Adv. 3, 1835–1843.

Sintra, T.E., Cruz, R., Ventura, S.P.M., Coutinho, J.A.P., 2014. Phase diagrams of ionic liquids-based aqueous biphasic systems as a platform for extraction processes. J. Chem. Thermodyn. 77, 206–213.

Sintra, T.E., Shimizu, K., Ventura, S.P.M., 2018. Enhanced dissolution of ibuprofen using ionic liquids as catanionic hydrotropes. Phys. Chem. Chem. Phys. 20, 2094–2103.
Steinberg, S.M., Poziomek, E.J., Engejmann, W.H., Rogers, K.R., 1995. A review of environmental applications of bioluminescence measurements. Chemosphere 30, 2155–2197.
Tsunashima, K., Kodama, S., Sugiya, M., Kunugi, Y., 2010. Physical and electrochemical properties of room-temperature dicyanamide ionic liquids based on quaternary phosphonium cations. Electrochim. Acta 56, 762–766.
Ullah, H., Wilfred, C.D., Shaharun, M.S., 2018. Ionic liquid-based extraction and separation trends of bioactive compounds from plant biomass. Separ. Sci. Technol. 54, 1–21.
Ventura, S.P.M., Marques, C.S., Rosatella, A.A., Afonso, C.A.M., Gonçalves, F., Coutinho, J.A.P., 2012. Toxicity assessment of various ionic liquid families towards Vibrio fischeri marine bacteria. Ecotoxicol. Environ. Saf. 76, 162–168.
Ventura, S.P.M., e Silva, F.A., Quental, M.V., Mondal, D., Freire, M.G., Coutinho, J.A.P., 2017. Ionic-liquid-mediated extraction and separation processes for bioactive compounds: past, present, and future trends. Chem. Rev. 117, 6984–7052.
Volpi, A.G., Girardini, M., Marchetto, D., Pantani, C., 2009. Microtox solid phase test : effect of diluent used in toxicity test. Ecotoxicol. Environ. Saf. 72, 851–861.
Wang, B., Shen, P., Zhu, W., Pang, Z., Dong, C., 2020a. Effect of ground wood particle size on biomass fractionation using p-toluenesulfonic acid treatment. Cellulose 27, 4043–4052.
Wang, W., Gu, F., Zhu, J.Y., Sun, K., Cai, Z., Yao, S., Wu, W., Jin, Y., 2020b. Fractionation of herbaceous biomass using a recyclable hydrotropic p–toluenesulfonic acid (p–TsOH)/choline chloride (ChCl) solvent system at low temperatures. Ind. Crop. Prod. 150, 112423.
Welton, T., 2015. Solvents and sustainable chemistry. Proc R Soc A Math Phys Eng Sci 471, 505–532.
Yang, M., Gao, X., Lan, M., Dou, Y., Zhang, X., 2019. Rapid fractionation of lignocellulosic biomass by p-TsOH pretreatment. Energy Fuel. 33, 2258–2264.
Zhou, Y., Boudesocque, S., Mohamadou, A., Dupont, L., 2015. Extraction of metal ions with task specific ionic liquids: influence of a coordinating anion. Separ. Sci. Technol. 50, 38–44.